



OPEN ACCESS

EDITED BY

Lucian Copolovici,
Aurel Vlaicu University of Arad, Romania

REVIEWED BY

Xiaoying Gong,
Fujian Normal University, China
Wei-Bin Wang,
Shenyang Agricultural University, China

*CORRESPONDENCE

Leonardo Montagnani
✉ leonardo.montagnani@unibz.it

RECEIVED 27 July 2024

ACCEPTED 27 November 2024

PUBLISHED 10 January 2025

CITATION

Singh N, Tagliavini M, Tomelleri E and
Montagnani L (2025) Multi-decadal tree-ring
stable isotope records of apple and pear trees
indicate coherent ecophysiological responses
to environmental changes in alpine valleys.
Front. Plant Sci. 15:1471415.
doi: 10.3389/fpls.2024.1471415

COPYRIGHT

© 2025 Singh, Tagliavini, Tomelleri and
Montagnani. This is an open-access article
distributed under the terms of the [Creative
Commons Attribution License \(CC BY\)](#). The
use, distribution or reproduction in other
forums is permitted, provided the original
author(s) and the copyright owner(s) are
credited and that the original publication in
this journal is cited, in accordance with
accepted academic practice. No use,
distribution or reproduction is permitted
which does not comply with these terms.

Multi-decadal tree-ring stable isotope records of apple and pear trees indicate coherent ecophysiological responses to environmental changes in alpine valleys

Nilendu Singh^{1,2}, Massimo Tagliavini¹, Enrico Tomelleri¹
and Leonardo Montagnani^{1*}

¹Faculty of Agricultural, Environmental and Food Sciences, Free University of Bolzano, Bolzano, Italy,

²Wadia Institute of Himalayan Geology, Dehradun, India

The ecophysiological and ecohydrological impacts of climate change and progressively increasing atmospheric carbon dioxide (CO₂) concentration on agroecosystems are not well understood compared to the forest ecosystems. In this study, we utilized the presence of old apple and pear trees in the alpine valleys of Northern Italy (maintained for cultural heritage purposes) to investigate climate-scale physiological responses. We developed long-term tree-ring stable isotopic records ($\delta^{13}\text{C}$ and $\delta^{18}\text{O}$) from apple (1976–2021) and pear trees (1943–2021). This allowed the reconstruction of key ecophysiological processes like the variations in intrinsic water use efficiency (*i*WUE), and we investigated how these trees responded to climate and CO₂ changes over decades. Results showed a slight declining trend in carbon discrimination ($\Delta^{13}\text{C}$) while intercellular CO₂ concentration (*C*_i) for both species has been increasing since the late 1980s. Concurrently both species exhibited a rising trend in *i*WUE, with apple trees demonstrating higher efficiency, which appears to be primarily driven by the CO₂-fertilization effect. The concomitant trends in tree-ring $\delta^{18}\text{O}$ suggested a relatively stable local hydroclimate during the study period with some species-specific responses. Analyses further revealed that minimum growing season temperature, not precipitation was the most significant factor influencing the rise in *i*WUE alongside with CO₂ fertilization effect. Analyses of species' $\delta^{13}\text{C}$ coupled with their respective $\delta^{18}\text{O}$ confirmed that the rise in *i*WUE was due to increased carbon assimilation rather than a decline in evapotranspiration. Moreover, coupled $\delta^{13}\text{C}$ – $\delta^{18}\text{O}$ analyses suggested increasing trends in carbon assimilation, with apple trees showing higher inter-decadal variations. These long-term records provide a unique opportunity to test and calibrate how these systems respond to recent and anticipated climate change.

KEYWORDS

dendrochronology, ecophysiology, WUE, climate-carbon response, Italian Alps

1 Introduction

The forest and agroecosystems in the European Alps play a very important role in providing food, goods, and ecosystem services (Stenger et al., 2009). However, concurrent climatic change and continually increasing atmospheric CO₂ concentration are expected to strongly affect the ecophysiology of these ecosystems, which could alter their productivity. The fertilizing effects of rising CO₂ levels, along with nitrogen depositions and increasing temperatures, have been shown to positively affect the productivity of European forests (Hyvönen et al., 2007; Giammarchi et al., 2017). Important studies that analyzed stable tree-ring isotopes across European forests have revealed valuable insights into forest ecosystem functioning and responses to climate change, including the CO₂-fertilization effect (Huang et al., 2024). The intrinsic water use efficiency (*i*WUE: ratio of photosynthesis to stomatal conductance) along with forest transpiration was found to increase over the 20th century with a consistent south-to-north gradient, which largely depended upon local growth limiting factors (Peñuelas et al., 2011). Across Europe, the strongest increase in *i*WUE was observed in the water-limited temperate forests in the central region (Saurer et al., 2014). Concerning the magnitude, mechanisms, and spatial patterns, the impact of climate change on European forests is quite diverse depending upon the geography and local growth limiting factors (Saurer et al., 2014; Frank et al., 2015).

Nevertheless, the response of tree physiology to increasing CO₂ levels is far from being a straightforward one, indeed it strongly depends on local conditions with a species-specific response (Huang et al., 2024). It could interact with other climate drivers, such as warming-induced soil drying and physiological acclimation to high CO₂ levels (Saurer et al., 2014; Frank et al., 2015). Consequently, a global analysis of tree-ring isotope datasets indicates diminishing CO₂-driven gains in *i*WUE, in which deciduous species contributed more than conifers to the recent slowdown (Adams et al., 2020). Particularly, European forests at the northern periphery show a progressively diminishing response to increasing CO₂ concentration (Waterhouse et al., 2004). Moreover, the debate on the relative roles of enhanced photosynthesis vs reduced stomatal conductance in the global trends of *i*WUE has been tried to settle by combining tree-ring δ¹³C and δ¹⁸O datasets with a water-carbon optimality model (Lin et al., 2022; Walker et al., 2021).

Conversely, the response of climate change including CO₂-fertilization effect on the physiological functioning of economically important agroecosystems is less explored. This is primarily because of the lack of old wild or cultivated trees having long-term tree-ring width or isotopic records. Tree-ring stable isotopic records (δ¹³C and δ¹⁸O) differ from classical dendrochronological variables (such as width) as they reflect more directly the plant's physiological response to climate and environmental variables (Wang et al., 2019). δ¹³C values depend on factors affecting the photosynthetic uptake of CO₂ and are mainly controlled by stomatal conductance and the rate of carboxylation during photosynthesis. Whereas, δ¹⁸O values are constrained by the isotopic ratio of the source water and locally integrate the stomatal response to vapor pressure deficit via leaf water enrichment, coupled with transpiration. These factors controlling isotopic fractionation are closely related to the

meteorological variables (McCarroll and Loader, 2004; Battipaglia et al., 2013; Gagen et al., 2022). In this context, tree isotopes provide precise, reliable, large-scale, and long-term information to advance our understanding of ecosystem functioning, carbon – water cycling and to reconstruct key metrics and processes for the decades preceding observational data (Babst et al., 2014). Moreover, dual isotope analysis (δ¹⁸O – δ¹³C) provides a physiological basis to understand carbon – water processes including stomatal conductance and the effect of climate warming and CO₂ – fertilization (Siegwolf et al., 2023). The physiological interpretation of tree-ring δ¹⁸O is indeed complex (Lin et al., 2022). Yet, it remains the only proxy in conjunction with δ¹³C, which could be used to reconstruct mechanisms through which *i*WUE changes in response to climatic drivers, including atmospheric CO₂ (Siegwolf et al., 2023).

In this study, we generated long-term stable isotope (δ¹³C and δ¹⁸O) records of unique and old apple (1976-2021) and pear trees (1943-2021), which constitute major agro-economic crops in the Italian Alps (Alto Adige, Northern Italy, Figure 1). The alpine valleys of the region is a major apple production center in the country, where we analyzed δ¹³C and δ¹⁸O chronologies to understand how these trees responded to climate and CO₂ changes over decades. This study specifically aims to reconstruct δ¹³C-based ecophysiological processes and carbon-water coupling process (*i*WUE) and to investigate long-term climate – carbon responses. This approach lays the foundation for using wood carbon-oxygen stable isotope analysis to understand the meteorological constraints on fruit tree production potential.

2 Materials and methods

2.1 Study sites and climate

The study sites are located in valleys of the eastern Alps in South Tyrol, Italy (Figure 1). This region is a major apple producer, boasting around 18,000 hectares of apple orchards that contribute roughly half of Italy's apple production. In the past, pear trees were also widely cultivated, but this practice declined significantly by the 1970s. Land previously used for pears now primarily houses apple orchards. Current apple yields in the region average around 55 tons per hectare. Due to the relatively short lifespan of apple and pear orchards (around 20-30 years), they are not ideal for studying long-term climate impacts. To address this challenge, we collaborated with experts from South Tyrolean Fruit Tree Cultivation Museum to access two rather unique sites featuring old veteran apple and pear trees maintained for cultural heritage purposes. The apple orchard, within the municipality of Lana (46.60° N, 11.16° E, 310 m asl), featuring trees of the variety “Gravenstein” grafted on seedling rootstocks, was established around 1976. The pear orchard is located in the municipality of Prato allo Stelvio (46.63° N, 10.61° E, 884 m asl). Trees of the variety “Bartlett”, grafted on seedling rootstocks, were planted between 1928 and 1938. The pear site sampling also included a monumental tree of more than 200 years old belonging to the variety “Pala Birne”. Both orchards have received regular management practices since their

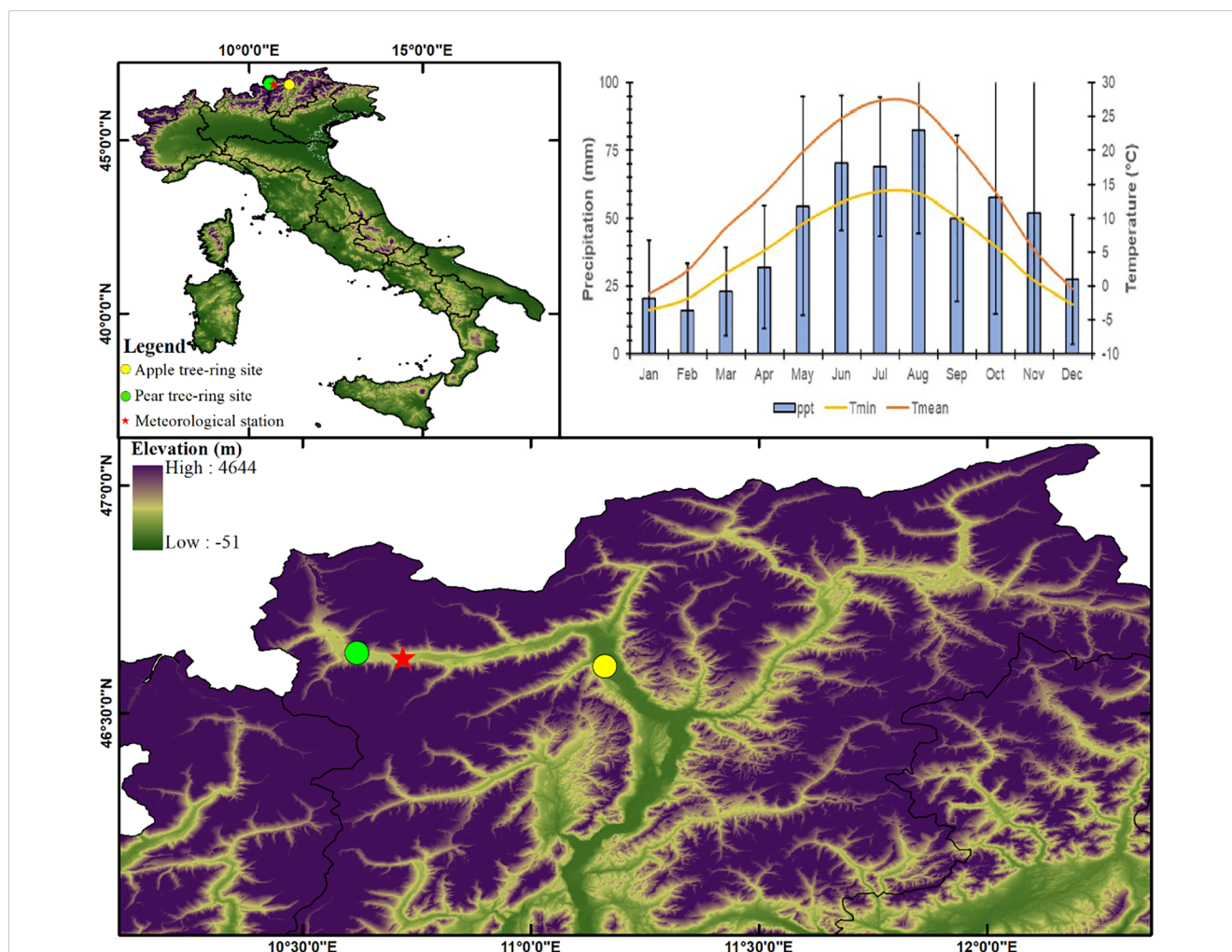


FIGURE 1

Location map of studied apple and pear orchards in the alpine valleys of the Italian Alps from where tree cores have been collected. The meteorological plot indicates regional climatology (Meteorological station: Silandro; Precipitation: 1981-2021; Temperature: 1988-2021).

establishment, including pruning, fertilization, irrigation, pest and disease control, and fruit harvesting. The soil in the sampling area has a sandy loam texture and is relatively fertile due to its high organic matter content.

Meteorological data from the Schlanders-Silandro station (46.62° N, 10.72° E, 698 m asl), located between the two sampling sites (Figure 1), suggests that the sites are energy-limited ecosystems, where temperature remains optimal only during the short growing season (April – September). These records indicate annual precipitation (1981 – 2021) in the range of 400 – 800 mm, of which, the growing season months (April – September) receive about 60% and the rest mostly as snowfall during winter. The mean annual temperature (1988 – 2021) varies between -1.2 and 27.3°C, which remains above 13°C during the growing season (Figure 1). The range of variation of minimum temperature is -3.5 to 14.0°C, which remains above 5°C during the growing season (Figure 1). In recent decades, temperature trends have generally been upward, with an overall warming trend observed across the region. The average temperature in Europe has increased by around 1.5°C since the pre-industrial era, and the warming trend has been more

pronounced in winter than in summer. According to the European Environment Agency, overall precipitation has remained relatively stable, with an increase of around 5% since the pre-industrial era.

2.2 Tree-ring stable isotope chronologies and computations

For each species, five trees were randomly selected and from each tree, two cores were extracted at 0.5 m from the ground using a 10 mm diameter increment borer. These increment cores were air-dried and glued on wooden supports. The cross-sectional surface of the cores was sanded by increasingly fine sandpapers until growth rings were visible and finally digitalized with a high-resolution scanner (2400 d.p.i.; Epson Expression 10000XL, Long Beach). A standard image was created for each sample and all images were saved into a graphic file format for further analysis. Subsequently, the determination of the tree ring width of each sample was performed with the Coo-recorder software (Cybis Elektronik &

Data AB, Saltsjöbaden, Sweden) at a precision level of 0.01 mm (García-Hidalgo et al., 2022).

We selected three individuals from each species based on the absence of biotic damages and on the chronological length for the isotopic analyses. Each year's growth-ring was cut using a sharp razor blade under the binocular microscope and pooling was performed for the individual tree rings of corresponding age. We utilized the whole-wood for the stable isotope analyses ($\delta^{13}\text{C}$ and $\delta^{18}\text{O}$) (Schollaen et al., 2017; Wieser et al., 2016). Stable isotope analyses were carried out at the Università degli studi della Campania "L. Vanvitelli" Dipartimento di Scienze e Tecnologie Ambientali Biologiche e Farmaceutiche, Caserta, Italy. The analytical precision was equal to or better than 0.2‰ for both the isotopes. The isotope ratios are presented in common δ -notation against international standard PDB and VSMOW respectively as:

$$\delta^{13}\text{C} = \left[\frac{\left(\frac{^{13}\text{C}}{^{12}\text{C}}\right)_{\text{sample}}}{\left(\frac{^{13}\text{C}}{^{12}\text{C}}\right)_{\text{PDB}}} - 1 \right] \times 1000 \text{ (‰)} \quad (1)$$

$$\delta^{18}\text{O} = \left[\frac{\left(\frac{^{18}\text{O}}{^{16}\text{O}}\right)_{\text{sample}}}{\left(\frac{^{18}\text{O}}{^{16}\text{O}}\right)_{\text{VSMOW}}} - 1 \right] \times 1000 \text{ (‰)} \quad (2)$$

Where, ($^{13}\text{C}/^{12}\text{C}$) sample and ($^{13}\text{C}/^{12}\text{C}$) PDB are heavy to light carbon isotope ratios in the wood sample and the standard (Vienna Pee Dee Belemnite), respectively. ($^{18}\text{O}/^{16}\text{O}$) sample and ($^{18}\text{O}/^{16}\text{O}$) VSMOW are heavy to light oxygen isotope ratios in the wood sample and the international standard (Vienna Standard Mean Ocean water) respectively.

Discrimination against ^{13}C ($\Delta^{13}\text{C}$, ‰) during carbon fixation by trees was computed by using atmospheric ($\delta^{13}\text{C}_{\text{atm}}$) and tree-ring ($\delta^{13}\text{C}_{\text{plant}}$) $\delta^{13}\text{C}$ as:

$$\Delta^{13}\text{C} = \frac{\delta^{13}\text{C}_{\text{atm}} - \delta^{13}\text{C}_{\text{plant}}}{1 + \delta^{13}\text{C}_{\text{plant}}} \quad (3)$$

Where, ($\delta^{13}\text{C}_{\text{atm}}$) and ($\delta^{13}\text{C}_{\text{plant}}$) are fractional differences in isotopic composition ($^{13}\text{C}/^{12}\text{C}$) in atmospheric CO_2 and that of tree-ring wood. We compiled $\delta^{13}\text{C}_{\text{atm}}$ from McCarroll and Loader (2004) up to the year 2004, and after that was derived from Belmecheri and Lavergne (2020) (<https://scrippsco2.ucsd.edu/data/>). A widely accepted procedure to correct tree-ring isotope chronology for the incorporation of isotopically light carbon released by the burning of fossil fuels and increasing CO_2 concentration was adopted (McCarroll and Loader, 2004). The correction procedure has the advantage of being an objective one as it effectively removes any declining trend in the $\delta^{13}\text{C}$ series post AD 1850, which is attributed to physiological response to increased atmospheric CO_2 concentrations (McCarroll and Loader, 2004).

Carbon isotopic discrimination ($\Delta^{13}\text{C}$) is related to intercellular CO_2 (C_i) and atmospheric CO_2 (C_a) concentration as:

$$\Delta^{13}\text{C} = a + (b - a) \left(\frac{C_i}{C_a} \right) \quad (4)$$

Where, 'a' is the fractionation factor during intercellular diffusion (-4.4‰), and 'b' is the fractionation factor during

carboxylation (-27‰) (Farquhar et al., 1982). The ratio of C_i and C_a was determined as:

$$\frac{C_i}{C_a} = \frac{\delta^{13}\text{C}_{\text{plant}} - \delta^{13}\text{C}_{\text{atm}} + a}{a - b} \quad (5)$$

or,

$$\frac{C_i}{C_a} = \frac{\Delta^{13}\text{C} - a}{b - a}$$

Using C_i and C_a values, intrinsic water use efficiency ($i\text{WUE}$) was calculated as:

$$i\text{WUE} = \frac{C_a - C_i}{1.6} \quad (6)$$

To substantiate our inferences, we computed a standardized carbon-to-oxygen isotope difference index for all species over the entire observation period, following the model of Scheidegger et al. (2000):

$$(C - O \text{ Difference Index})_n = (\delta^{13}\text{C}_{\text{zscore}})_n - (\delta^{18}\text{O}_{\text{zscore}})_n \quad (7)$$

Here, n is the year. Both corrected $\delta^{13}\text{C}$ and $\delta^{18}\text{O}$ chronologies were transformed into z-scores (based on the long-term mean and std. dev.) and analyzed in pairs for each crop. This index allows tracking year-by-year changes in trees' physiological conditions induced by changes in stomatal conductance and photosynthetic capacity. The index assumes values close to 0 when both isotope ratios show similar values, indicating either enhanced stomatal conductance (both isotopic values are negative) or reduced stomatal conductance (both isotopic values are positive). Positive index values indicate high photosynthetic capacity (high $\delta^{13}\text{C}$ and low $\delta^{18}\text{O}$), while negative values indicate low photosynthetic capacity (low $\delta^{13}\text{C}$ and high $\delta^{18}\text{O}$) (Scheidegger et al., 2000; Siegwolf et al., 2023).

2.3 Statistical analyses

To understand relationships between $\delta^{13}\text{C}$ -based processes (C_i , $\Delta^{13}\text{C}$, $i\text{WUE}$) in the two species and the regional climate (Precipitation and Temperature: Mean, Max., Min.), simple Pearson correlations were applied with a response-function approach. The confidence intervals of correlations were analyzed at 95% and 99% levels. This helped to investigate the correlations with monthly climatic averages in the species. To corroborate and stabilize these relations further, we plotted 3-month moving correlation coefficients between physiological processes and monthly hydroclimatic data (precipitation: 1982-2021; temperature: 1988-2021). The response function analysis for the species was plotted from October of the previous growth year to September of the current year (pOct-Sep). To test the relative importance of climate parameters including atmospheric CO_2 levels, multiple linear regression models with $i\text{WUE}$ as the response variables, and temperature (mean, max, min), precipitation, and atmospheric CO_2 as continuous predictor variables, were built.

To test the significance of the slopes (p -values), we first computed Mean Square Error (MSE) as: $MSE = (1 - R^2) \times Var(y)$.

Then, the Standard Error (SE) of the slope was computed as: $\sqrt{\frac{MSE}{(n-1) \times Var(x)}}$; and the t-statistic was calculated as: $t = \frac{slope}{SE}$.

Finally, using the t-distribution, we calculated the two-tailed *p*-value for the respective t-statistics and degrees of freedom ($df = n - 2$).

We used 'lm' function from the R statistical computing environment (R development Core team, 2015). The relative importance of significant terms was obtained by applying function 'calc.relimp' using default options (Supplementary Table S1). The process reconstructions were standardized using Z-scores and smoothed with a 3-year running mean to assess common signals.

3 Results and discussion

3.1 Carbon isotope chronologies and climate response

Over the study period, raw $\delta^{13}\text{C}$ in tree-rings of pear (1943–2021) and apple (1976–2021) species exhibited a slight decreasing trend (Figure 2). The break-point analysis identifies the year of change in carbon isotopic composition in the species as the year 1987–88. Therefore, 1990 is assigned as a reference year for the analyses. For the common period, inter-species correlation was moderate at the inter-annual scale ($r = 0.398$, $p < 0.001$), which

indicates the predominance of both species-specific and site-specific local effects on the assimilation process. The mean $\delta^{13}\text{C}$ value of apple trees was -25.6‰ (std. dev.: 0.40‰), while for the pear trees, it was $\sim 1.0\text{‰}$ lower ($-26.6 \pm 0.32\text{‰}$) (Figure 2A; Table 1). This difference suggests a higher level of assimilation rate (isotope discrimination) in pear trees (Figure 2B). However, pear and apple trees have reportedly similar daily radiation use efficiency (Auzmendi et al., 2013). The long-term mean of $\delta^{13}\text{C}$ (corrected for atmospheric CO_2 increase) in apple trees was $-23.5 \pm 0.6\text{‰}$, which increased slightly ($-23.2 \pm 0.52\text{‰}$) after 1990. The long-term mean for the pear trees ($-25.1 \pm 0.72\text{‰}$) increased by $\sim 1\text{‰}$ after 1990 ($-24.3 \pm 0.42\text{‰}$) (Supplementary Figure S1). Considering the changes in atmosphere-to-plant $^{13}\text{CO}_2$ discrimination ($\Delta^{13}\text{C}$), we found a higher ($\sim 2.0\text{‰}$) level of discrimination in pear trees, which showed a similar temporal pattern to that of apple trees (Figure 2; Table 1). The corrections of the carbon isotope series of the two species for the physiological responses to increasing concentrations of atmospheric CO_2 are illustrated in the supplementary figure (Supplementary Figure S1).

A rising trend in intercellular CO_2 (C_i) in the two species was noted during the observation period. The mean C_i value of the apple tree was $223 \pm 10.3 \mu\text{mol mol}^{-1}$, while for the pear trees, it was $233 \pm 13.6 \mu\text{mol mol}^{-1}$ (Table 1). Prior to 1990, the mean C_i of apple trees was $207 \mu\text{mol mol}^{-1}$ (range: $181 - 230 \mu\text{mol mol}^{-1}$), which

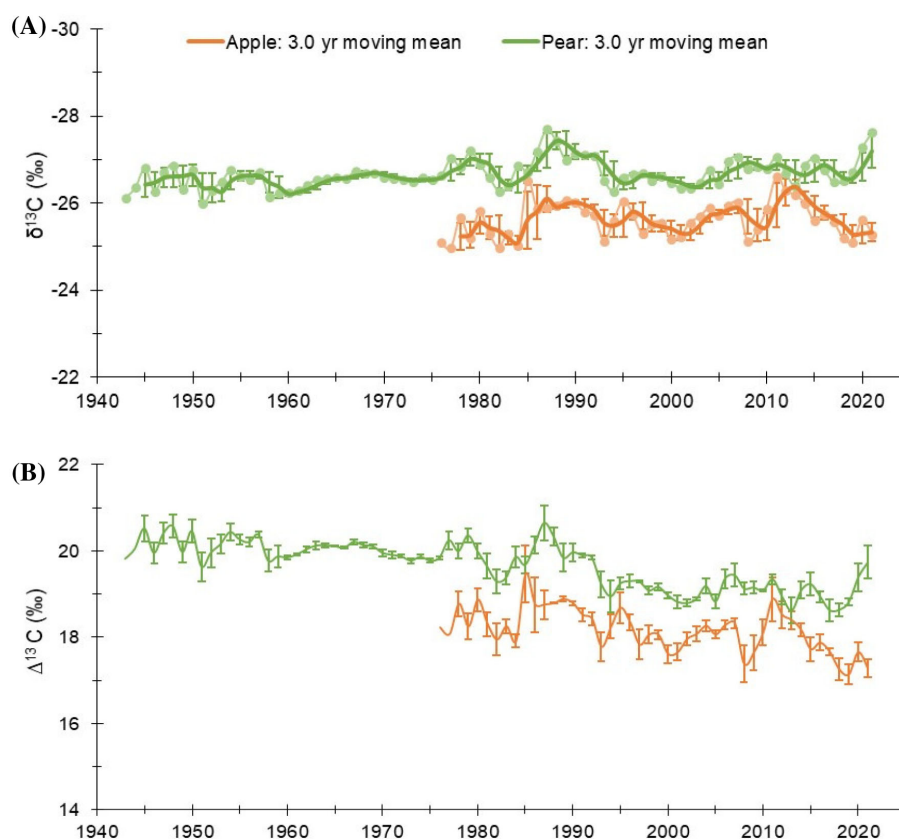


FIGURE 2

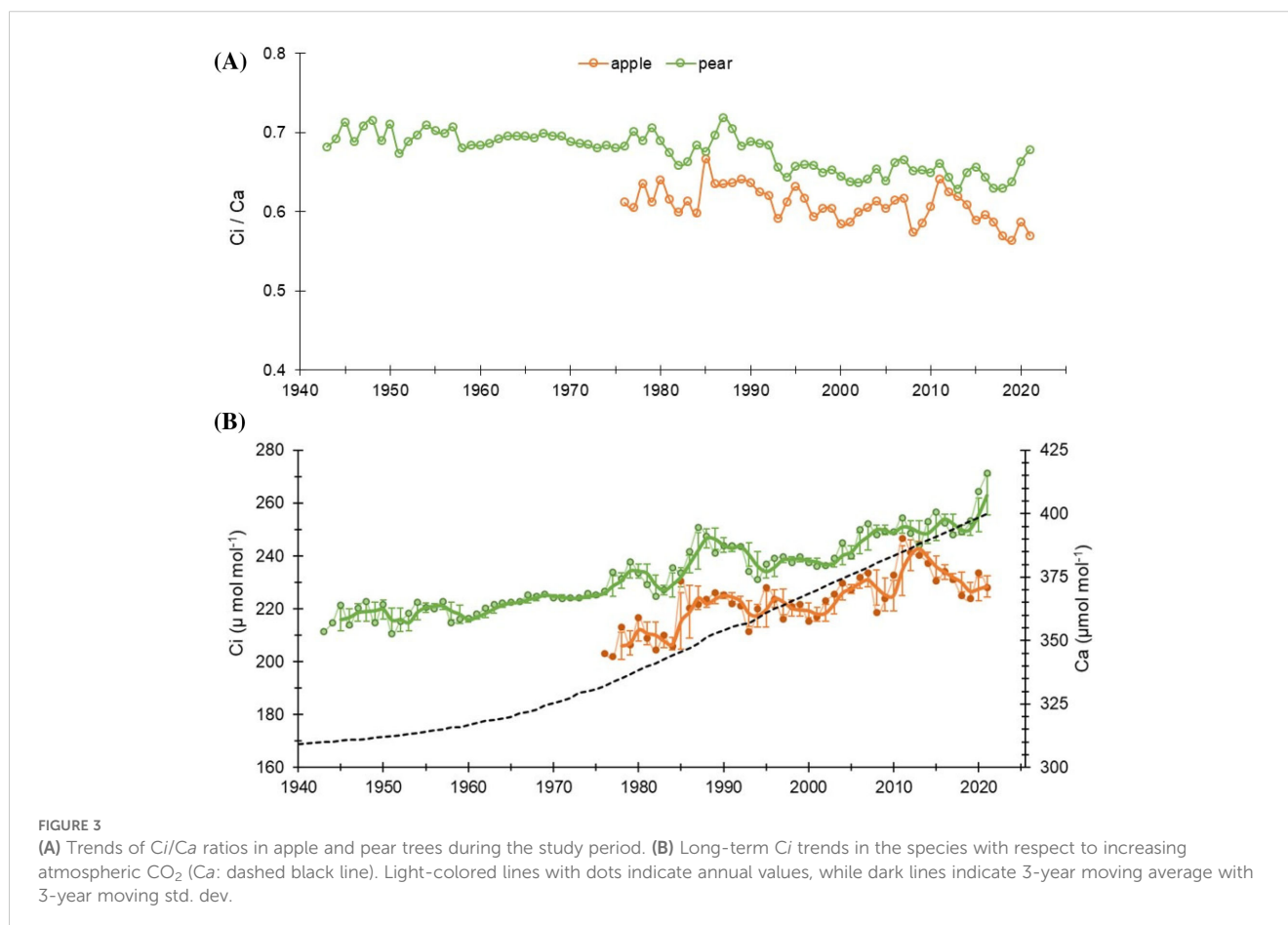
(A) $\delta^{13}\text{C}$ chronologies of pear and apple trees (Pear: 1943 – 2021; Apple: 1976 – 2021). Faded line with dots denote annual values. Colored dark lines represent three year moving mean with three-year moving std. dev. (B) Annual atmosphere-to-plant $^{13}\text{CO}_2$ discrimination ($\Delta^{13}\text{C}$) trends in the species with 3-year moving std. dev.

TABLE 1 Descriptive statistics of tree-ring variables of the two tree species.

Species	Variables	Minimum	Maximum	Mean \pm SE	SD
Apple (1976-2021)	$\delta^{13}\text{C}$ (‰)	-26.6	-24.9	-25.6 ± 0.08	0.4
	$\Delta^{13}\text{C}$ (‰)	17.1	19.4	18.0 ± 0.07	0.56
	C_i ($\mu\text{mol mol}^{-1}$)	202.0	247.0	223.0 ± 1.96	10.3
	$i\text{WUE}$ ($\mu\text{mol mol}^{-1}$)	72.0	108.2	89.5 ± 1.23	8.8
	C_i/Ca	0.56	0.66	0.60 ± 0.003	0.02
	$\delta^{18}\text{O}$ (‰)	24.1	29.0	26.3 ± 0.2	1.25
Pear (1943-2021)	$\delta^{13}\text{C}$ (‰)	-27.7	-26.0	-26.6 ± 0.03	0.32
	$\Delta^{13}\text{C}$ (‰)	18.6	20.6	19.6 ± 0.06	0.53
	C_i ($\mu\text{mol mol}^{-1}$)	210.5	264.0	233.0 ± 1.47	13.6
	$i\text{WUE}$ ($\mu\text{mol mol}^{-1}$)	55.3	91.5	70.4 ± 1.19	10.5
	C_i/Ca	0.63	0.72	0.67 ± 0.002	0.02
	$\delta^{18}\text{O}$ (‰)	23.5	28.4	25.9 ± 0.11	0.99

increased to $227 \mu\text{mol mol}^{-1}$ ($211 - 247 \mu\text{mol mol}^{-1}$). While, for the pear trees, the mean C_i before and after 1990 was $225 \mu\text{mol mol}^{-1}$ ($211 - 251 \mu\text{mol mol}^{-1}$) and $245 \mu\text{mol mol}^{-1}$ ($231 - 264 \mu\text{mol mol}^{-1}$), respectively (Figure 3). The trends in intercellular CO_2 (C_i) to atmospheric CO_2 (Ca), i.e., C_i/Ca ratio in both species were analogous to the trends in $\Delta^{13}\text{C}$. Nonetheless, a declining trend in

both species is noticeable after 1990. Prior to 1990, the ratio for the apple trees was 0.62 ($0.59 - 0.66$), which decreased to 0.60 ($0.56 - 0.64$). While, in the pear trees the ratio before and after 1990 was 0.69 ($0.66 - 0.71$) and 0.65 ($0.63 - 0.69$), respectively. Fitted regression slopes for the C_i/Ca ratio ($p < 0.05$) in apple and pear trees prior to 1990 were 0.0021 ($R^2 = 0.2$) and -0.0003 ($R^2 = 0.087$),



respectively. After 1990, magnitude of the slopes becomes more negative (Apple: -0.0011 , $R^2 = 0.25$; Pear: -0.0009 , $R^2 = 0.28$). Out of three theoretical scenarios of Ci/Ca ratios to CO_2 rise (Panthi et al., 2020), a positive slope in apple trees suggests a ' $Ca - Ci = \text{constant}$ ' scenario prior to 1990 that changed to ' $Ci = \text{constant}$ ' scenario after 1990. Conversely, the response of pear trees appears to be a ' $Ci = \text{constant}$ ' scenario throughout the observation period. These results probably suggest a varying physiological response of tree species to atmospheric CO_2 rise (Figure 3).

The $\Delta^{13}C$ discrimination at the plant level is controlled by Ci/Ca ratio. This ratio could decline either because of low stomatal/mesophyll conductance to CO_2 associated with water stress or low temperatures, or due to a high assimilation rate (McCarroll and Loader, 2004). At our sites, in the alpine valleys with frequent irrigation, water cannot be assumed to be a limiting factor. Growth at higher latitudes is generally limited by suboptimal temperatures for xylogenesis (i.e., formation of water conductive tissue), which remains almost optimal during the growing season. In energy-limited ecosystems at higher latitudes, climate warming may improve tree-water status where xylogenesis is temperature-limited and given that sufficient water is available. Therefore, increasing assimilation rates due to rising CO_2 levels could be another reason for the observed declining Ci/Ca ratio in recent decades. The effect of CO_2 fertilization has been observed globally, which is quite pervasive in European forests, particularly over the northern ecosystems (Mathias and Thomas, 2021; Waterhouse et al., 2004; Saurer et al., 2014; Frank et al., 2015).

Hydro-climate response function: the Pearson correlation with a response function approach demonstrates the relationship between species' physiological processes ($\delta^{13}C$, $\Delta^{13}C$, and Ci) and monthly hydroclimatic data (precipitation and temperature: mean, maximum, and minimum). To corroborate and stabilize these monthly relations, we plotted 3-month moving correlation coefficients (precipitation: 1982-2021; temperature: 1988-2021) (Figure 4). The response function analysis for the $\delta^{13}C$ - precipitation relationship from October of the previous growth year to September of the current year (pOct-Sep) revealed non-significant correlations. The relationship confirms that water is not a limiting factor in these orchards, having provision of irrigation, especially for the apple trees. For this reason, at the beginning of the growing season (March-May) we observed an enhanced positive correlation for the pear trees. In contrast and irrespective of the seasons, $\delta^{13}C$ - precipitation relationship for the apple trees was non-significant (Figure 4A). Likewise, $\Delta^{13}C$ - and Ci - precipitation relationship during peak growing season (June-October) was significant for the pear trees but non-significant for the apple trees having inverse correlations (Figures 4B, C). Yet, Pearson correlations and 3-month moving correlations with temperature indicated that the latter has a major control on the species' ecophysiological processes (Figures 4D-F). The $\delta^{13}C$ - temperature (mean) relationship was non-significant for both species (Figure 4D). Nevertheless, we observed significant, $\Delta^{13}C$ - and Ci - mean temperature correlations across the months for both species (Figures 4E, F). Particularly, the influence of minimum temperature on $\Delta^{13}C$ and Ci was prominent during the entire growing season (March - October) (Supplementary Figures S2A-C). Whereas, maximum temperature appears to affect these processes

during the start of the growing season (April-June) (Supplementary Figures S2D-F). The relationships between temperature (Min., Max.) and $\delta^{13}C$, $\Delta^{13}C$, and Ci have been detailed in the supplementary figure (Supplementary Figures S2A-F).

3.2 Temporal trends in oxygen isotope series and climate response

Oxygen isotope in the tree-rings complemented with respective $\delta^{13}C$ values, remains the only proxy with proven potential to decipher a comprehensive picture of past and current ecophysiological status (Battipaglia et al., 2013; Nock et al., 2011; Siegwolf et al., 2023). Consequently, we have taken into account the $\delta^{18}O$ chronologies of the trees (Figure 5). The mean $\delta^{18}O$ value of pear trees (1943 - 2021) was 25.9 ± 0.99 ‰ (Coefficient of Variation (CV): 3.8%), while for the apple trees (1976 - 2021), it was ~ 1.0 ‰ higher (26.3 ± 1.25 ‰) with a higher CV (5.6%) (Table 1). Prior to 1990, the mean $\delta^{18}O$ of apple trees was 25.8 ‰ (range: 24.3 - 28.0 ‰), which showed a rising trend after 1990 with a similar range of variation. While, for the pear trees, the mean $\delta^{18}O$ before 1990 was 26.3 ‰ (24.5 - 28.4 ‰), which dropped to 25.2 ‰ (23.5 - 26.3 ‰) since then (Figure 5A). The mean difference between species indicates a higher level of oxygen isotope discrimination and evapotranspiration in pear trees relative to the apple trees. At the same vapor pressure deficit, leaves with high transpiration rates are known to become isotopically enriched in heavy isotopes as compared to leaves having low transpiration (McCarroll and Loader, 2004; Battipaglia et al., 2013). The optimal transpiration rate coupled with the use of enriched surface irrigated water by the apple trees and differences in the stomatal conductance could be responsible for such an ^{18}O enrichment offset. Moreover, because of limited evaporation, groundwater is less enriched (compared to surface water) and the probable use of this less enriched groundwater by the pear trees (having greater tree height and rooting depth) is reflected in its stable time series having lower CV (Figure 5A) and $\delta^{13}C$ - precipitation relationship (Figure 4A). However, a decline (after 1990) in ^{18}O enrichment (~ 1.0 ‰) in pear trees could be linked to increasing precipitation trend and irrigation provisioning.

Due to the above reasons, response function analysis for the monthly $\delta^{18}O$ - precipitation relationship (pOct-Sep) showed opposite correlations in the species (Figures 5B, C). Cross-correlations of $\delta^{18}O$ chronology of pear trees with precipitation revealed a strong positive relationship during the start of the growing season (March-May), which becomes negative during peak growing season (June-October). The $\delta^{18}O$ - precipitation relationship for the apple trees, on the contrary, was opposite to that of the pear trees and insignificant throughout the growing season (March-October) (Figure 5B). Similarly, correlations with mean temperature indicated opposite but a major control on species' ecophysiological processes associated with ^{18}O enrichment, particularly during peak growing season (June-October). For this period, the correlation was significantly positive and negative for apple and pear trees, respectively (Figure 5C). In contrast, during March-May, correlation was negative in both species but remained statistically insignificant. Both Pearson and 3-month moving correlations between minimum temperature and $\delta^{18}O$ have been

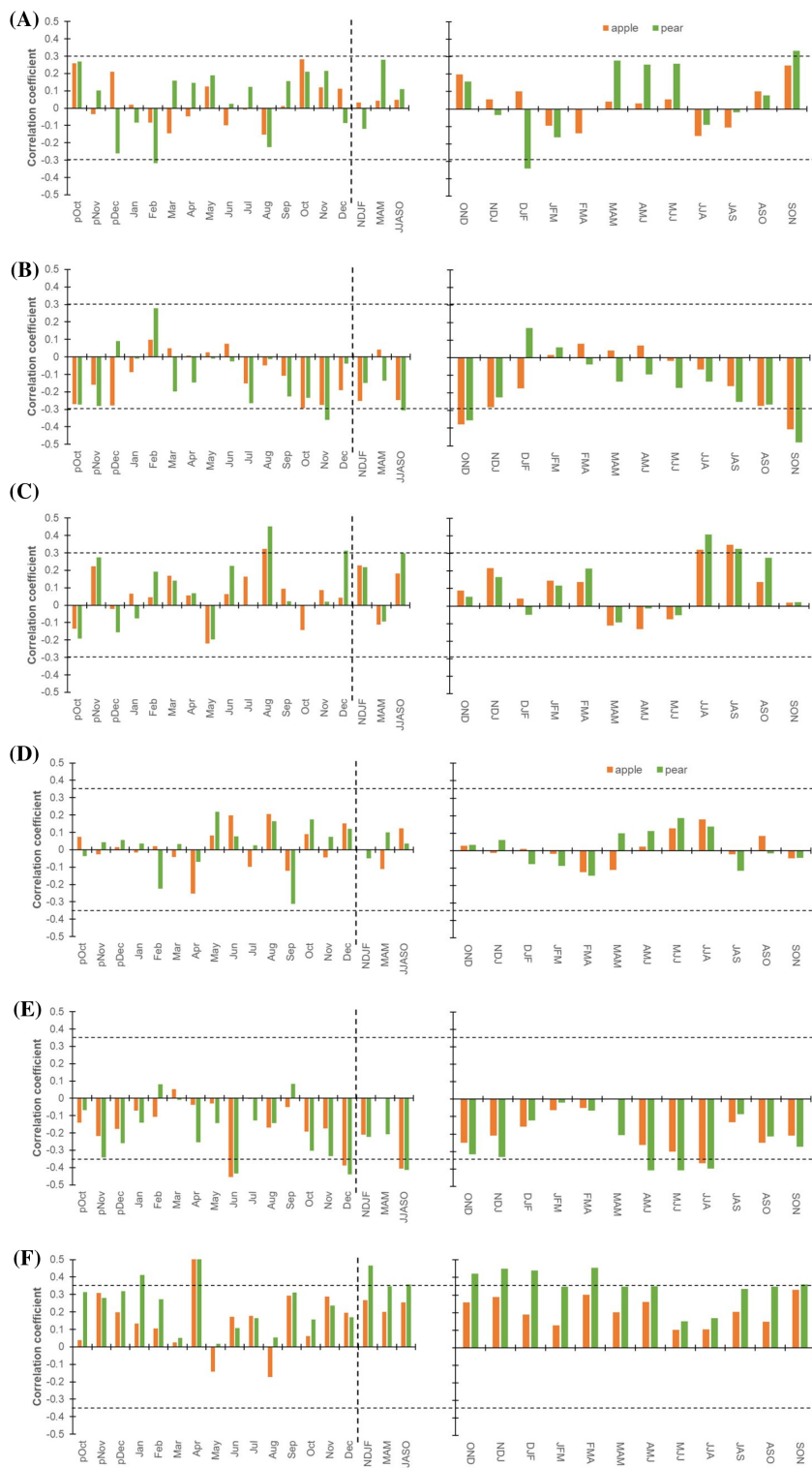


FIGURE 4

Hydro-climatic response function for Apple (orange) and Pear (green). **(A)** Monthly (left panel) correlations between $\delta^{13}\text{C}$ time series of species and precipitation (1981-2021). The corresponding right panel indicates three-month moving correlation coefficients between $\delta^{13}\text{C}$ and precipitation. **(B)** Monthly (left panel) and three-month moving (right panel) correlations between $\Delta^{13}\text{C}$ and precipitation. **(C)** Monthly (left panel) and three-month moving (right panel) correlations between species' C_i chronologies and precipitation. **(D)** Monthly (left panel) correlations between $\delta^{13}\text{C}$ chronologies of species and mean temperature (1988-2021). The corresponding right panel indicates three-month moving correlation coefficients between $\delta^{13}\text{C}$ and mean temperature. **(E)** Monthly (left panel) and three-month moving (right panel) correlations between species $\delta^{13}\text{C}$ values and mean temperature. **(F)** Monthly (left panel) and three-month moving (right panel) correlations between species C_i chronologies and mean temperature. The dotted horizontal line indicates a 95% confidence level. The dashed vertical line delimits months with seasonal aggregates. Prefix "p" before the months denotes the months of the previous growth year. The hydro-climatic response of species' $\delta^{13}\text{C}$, $\Delta^{13}\text{C}$ and C_i to minimum and maximum temperature has been illustrated in [Supplementary Figure S2](#).

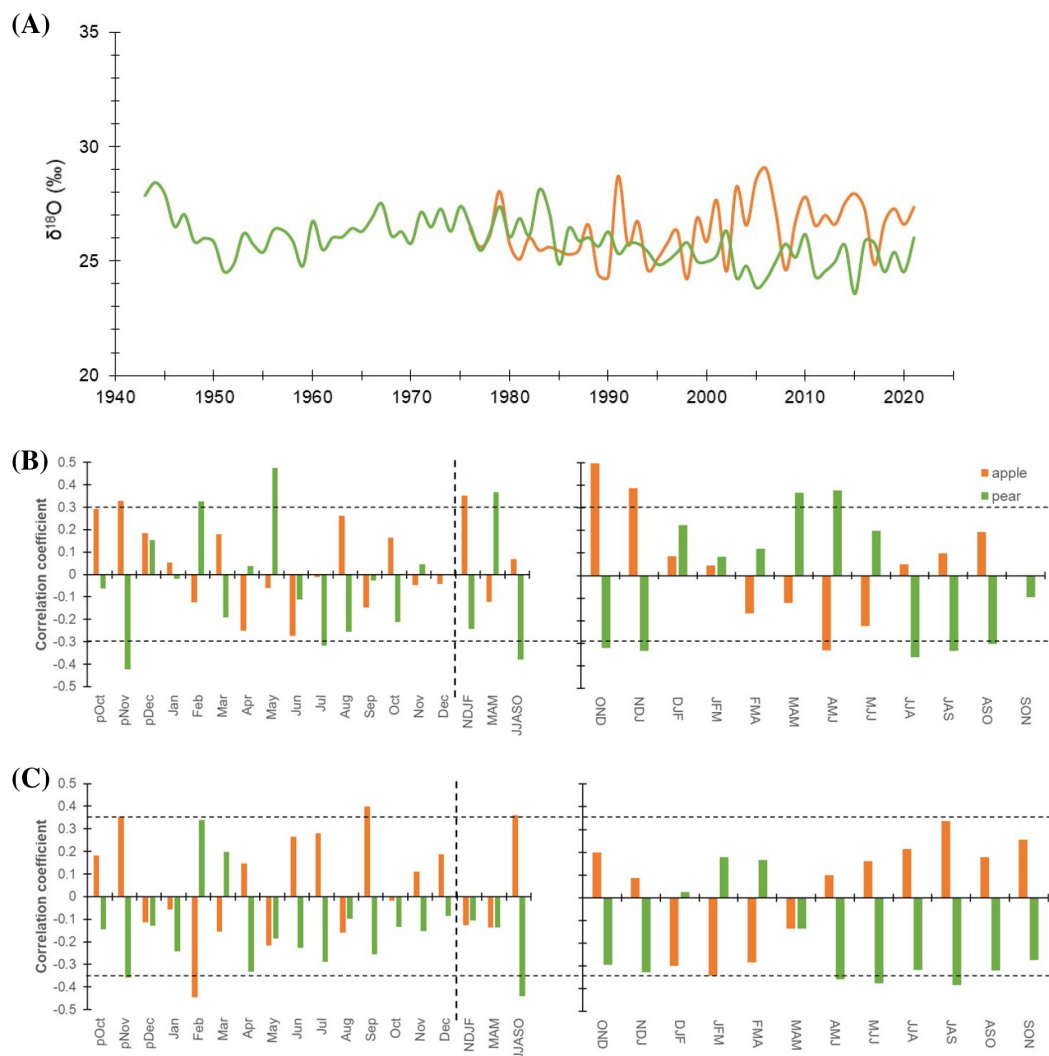


FIGURE 5

(A) $\delta^{18}\text{O}$ isotope chronologies of apple (orange line) and pear (green line) tree species. (B) Monthly (left panel) correlations between $\delta^{18}\text{O}$ chronologies of species and precipitation (1981–2021). The corresponding right panel indicates three-month moving correlation coefficients between $\delta^{18}\text{O}$ and precipitation. (C) Monthly (left panel) and three-month moving (right panel) correlations between species' $\delta^{18}\text{O}$ chronologies and mean temperature (1988–2021). The dotted horizontal line indicates a 95% confidence level. The dashed vertical line delimits months with seasonal aggregates. Prefix "p" before the months denotes the months of the previous growth year. The response of species' $\delta^{18}\text{O}$ to minimum and maximum temperature has been illustrated in [Supplementary Figure S3](#).

detailed in the supplementary figure ([Supplementary Figures S3A, B](#)), which reflects greater but opposite response for the two species during peak growing season (June–October). On the contrary, the impact of maximum temperature was minimal. Modelling studies indicate that tree-ring $\delta^{18}\text{O}$ values integrate signals from three primary factors: source water $\delta^{18}\text{O}$, evaporative enrichment of ^{18}O in leaf water, and biochemical fractionation during organic matter synthesis. Consequently, tree-ring $\delta^{18}\text{O}$ signals vary as a function of temperature, relative humidity, precipitation, water sources, and regional climate conditions ([Barbour, 2007](#); [Gessler et al., 2014](#); [Kahmen et al., 2011](#)). Based on the premise that tree roots take up soil water without fractionation, a major part of the isotopic signature in tree rings should reflect the variation in precipitation or hydroclimatic conditions ([Farquhar et al., 2007](#); [Lehmann et al., 2018](#); [Roden et al., 2005](#)). However, depending upon the local

humidity condition, species-specific ecophysiological processes and responses (e.g.: isotopic composition of soil water, leaf-water enrichment, and oxygen isotope exchange reactions of photosynthates with water) may have a considerable effect on tree ring $\delta^{18}\text{O}$ values ([Baker et al., 2016](#); [Lehmann et al., 2018](#)), as revealed in our study.

3.3 Temporal trends in water use efficiency and climate controls

Broadly, an increasing trend in $i\text{WUE}$ was observed during the study period in both species that raised sharply after the 1990s ([Figure 6](#)). The mean $i\text{WUE}$ of the apple tree was $88.5 \pm 9.0 \mu\text{mol mol}^{-1}$, while for the pear trees, it was lower at $70.3 \pm 10.5 \mu\text{mol mol}^{-1}$.

Prior to 1990, the mean *i*WUE of apple trees was $80.2 \mu\text{mol mol}^{-1}$ ($72 - 86 \mu\text{mol mol}^{-1}$), which increased to $93.6 \mu\text{mol mol}^{-1}$ ($80 - 108 \mu\text{mol mol}^{-1}$). In contrast, for the pear trees, the mean *i*WUE before and after 1990 was $62.6 \mu\text{mol mol}^{-1}$ ($55 - 73 \mu\text{mol mol}^{-1}$) and $81.8 \mu\text{mol mol}^{-1}$ ($69 - 91 \mu\text{mol mol}^{-1}$), respectively. During the observation period, mean *i*WUE of the apple trees was higher than that of the pear trees ($\sim 18 \mu\text{mol mol}^{-1}$), which after 1990 increased by 15.5 and 30.6% respectively for apple and pear trees (Table 1). For the common period, inter-species correlation was significantly high ($r = 0.82$, $p < 0.001$), which probably indicates the predominant control of climate on species' ecophysiological process.

Moreover, it would be informative to note that long-term gains in *i*WUE by vegetation are usually overestimated (Gong et al., 2022). To provide a more accurate assessment, it is crucial to account for post-photosynthetic fractionations and mesophyll conductance, which influence CO_2 diffusion to carboxylation sites (Gimeno et al., 2021; Gong et al., 2022; Ma et al., 2021). Our *i*WUE calculations, based on a linear model of photosynthetic ^{13}C discrimination ($\Delta^{13}\text{C}$), do not fully capture long-term structural and physiological acclimations. Therefore, we advocate for the adoption of advanced models that should incorporate post-photosynthetic fractionations and mesophyll conductance as well as photorespiration to mitigate errors in estimating *i*WUE from $\Delta^{13}\text{C}$ across vegetation types.

Nevertheless, to elaborate on the climatic controls of *i*WUE, we performed response function analysis on *i*WUE chronologies and monthly hydroclimatic datasets. For both species, major hydroclimatic variables (temperature and precipitation) showed positive relations with *i*WUE (Figures 6B, C). During the beginning of the growing season (March-May), *i*WUE – precipitation relationship was negative ($p > 0.05$) for the species that turned to positive correlations during the peak growing season (June-October) (Figure 6B). Cross-correlations with mean temperature revealed a strong positive correlation during peak growing season in both species, which was insignificantly low during March to May (Figure 6C). Similarly, with respect to minimum and maximum temperature, we noted a higher influence of minimum temperature on *i*WUE during peak growing season in both species (Supplementary Figures S4A, B).

Furthermore, stepwise regression between annual and 5-year mean *i*WUE (as dependent variable) and mean temperature (Tmean), precipitation (Ppt), and atmospheric CO_2 concentrations (CO_2) (as independent variables) were employed to assess the explanatory power of climate variables. In both species, annual CO_2 explained more than 70% of the variability. Whereas, 5-year mean CO_2 explained more than 90% of the variability in *i*WUE. Analyses further reveal that Tmean is the second most important variable, while precipitation has a minimal impact on species' *i*WUE (Supplementary Table S1). Several studies have inferred that rising atmospheric CO_2 levels do not always imply enhanced photosynthetic rate and tree growth (Nock et al., 2011; Rahman et al., 2020; Van Der Sleen et al., 2015), with species-specific responses. We also observed species-specific responses and noted a differential response of species' *i*WUE to atmospheric CO_2 (*Ca*) (Figure 6D). The regression coefficient in apple trees ($R^2 = 0.76$) was lower than that of the pear trees ($R^2 = 0.91$). Results further suggest a

slightly higher sensitivity of apple trees to rising *Ca* (slope: 0.38). However, a lower regression coefficient in apple trees indicates the possible role of other environmental factors particularly soil moisture (via stomatal regulation) in influencing their *i*WUE response. On the other hand, pear trees' *i*WUE appears more tightly correlated with atmospheric CO_2 levels (higher R^2) possibly due to their access to relatively invariable source water (groundwater), but having a slightly lower slope (0.35). Despite this, both species have similar intercepts (Apple: -50.89 and Pear: -50.64), suggesting comparable baseline *i*WUE in the context of CO_2 response. This implies that both species started from a similar baseline, but their responses to rising CO_2 levels have diverged.

In conclusion, both species have responded to rising CO_2 levels, with apple trees showing higher sensitivity as well as variability to environmental changes. Pear trees, on the other hand, have exhibited a more predictable and consistent response. It's possible that apple trees may have reached a threshold in their ability to increase WUE as CO_2 rises (Figure 6D). This information is valuable for predicting how these species may adapt to future environmental conditions, especially in regions with fluctuating water availability.

3.4 Temporal trends in species' dual isotope ($\delta^{13}\text{C} - \delta^{18}\text{O}$) series

Tree-ring $\delta^{18}\text{O}$, in combination with $\delta^{13}\text{C}$, is a powerful proxy to decipher a comprehensive picture of past and current ecophysiological status (Battipaglia et al., 2013; Nock et al., 2011; Siegwolf et al., 2023). Therefore, we computed carbon-to-oxygen isotope difference index for both species (Figure 7A). This difference serves as an indicator of the trees' physiological conditions related to changes in stomatal conductance and photosynthetic capacity (Scheidegger et al., 2000).

The C-to-O difference index for apple trees exhibits an increasing trend from the late 1970s onwards, with a more pronounced positive shift after the year 2000. The index also shows considerable year-to-year variability. In the early years (1976-1980), values fluctuate around the zero line, indicating a balance between low stomatal conductance and high photosynthetic capacity. From 1980 onwards, periods of high photosynthetic capacity (positive index values) appear more frequent and sustained, likely reflecting the irrigation effect. In recent years (2000-2021), the index mostly remained positive, indicating a generally high photosynthetic capacity for apple trees, despite occasional dips around 2010 and 2015.

The index for pear trees shows an overall increasing trend over the entire period. There is a clear positive shift around the late 1980s, aligning with the apple tree index. However, the species' pattern briefly diverged during the 2010s when $\delta^{13}\text{C}$ levels were stable and $\delta^{18}\text{O}$ values were high in apple trees (Figures 2, 5). Similar to apple trees, pear trees exhibit considerable inter-annual variability. The period before 1980 shows more frequent negative values, indicating periods of low photosynthesis, likely induced by stomatal limitations given limited irrigation provisioning. Post-1980, positive values become more dominant, suggesting an

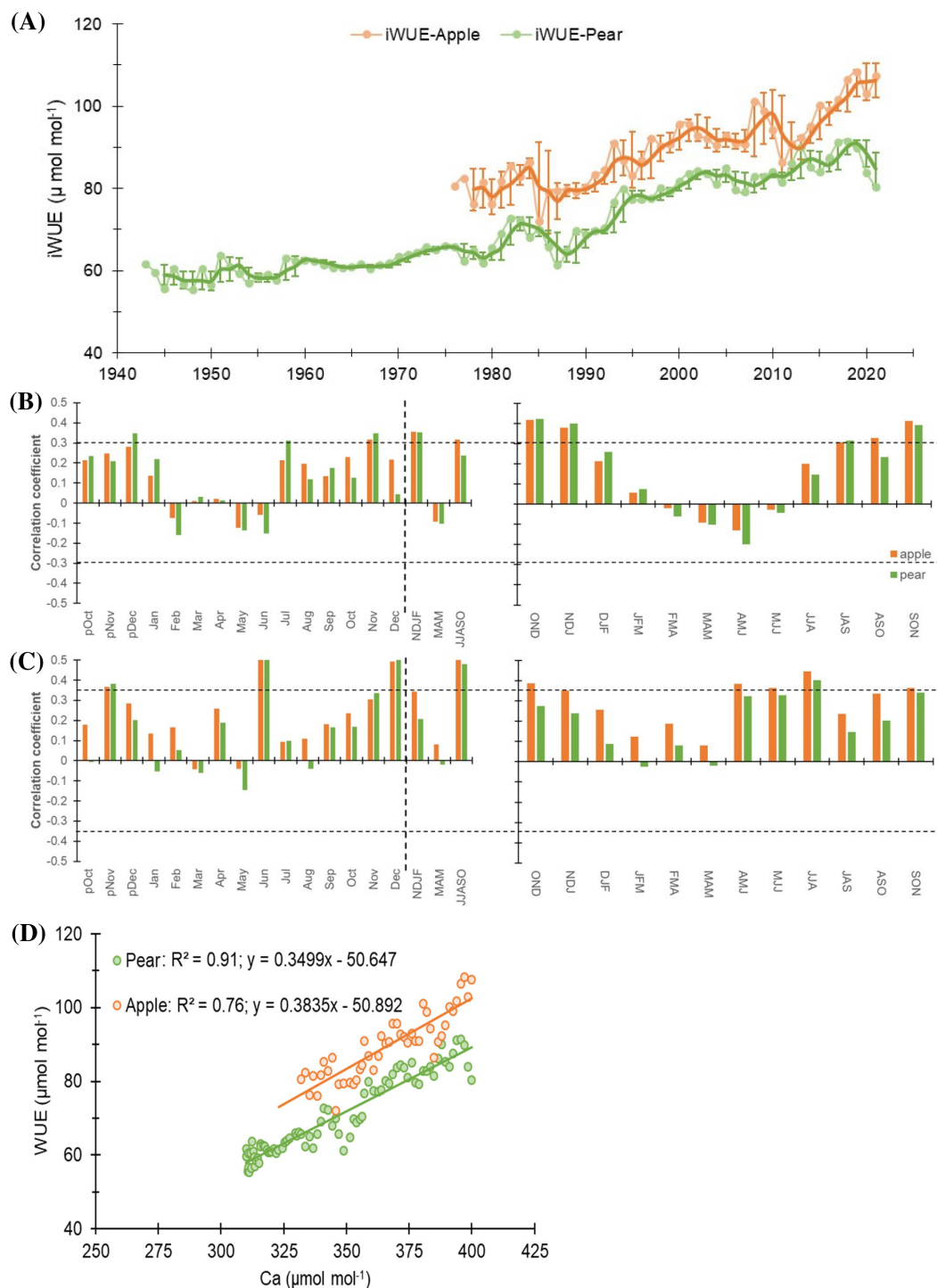


FIGURE 6
(A) iWUE time series of Apple and Pear. Light-colored lines with dots indicate annual values, while dark lines indicate 3-year moving average with std. dev. **(B)** Monthly (left panel) correlations between iWUE time series of species and precipitation (1981-2021). The corresponding right panel indicates three-month moving correlation coefficients between them. **(C)** Monthly (left panel) and three-month moving (right panel) correlations between species' iWUE time series and mean temperature (1988-2021). The dotted horizontal line indicates a 95% confidence level. The dashed vertical line delimits months with seasonal aggregates. Prefix "p" before the months denotes the months of the previous growth year. The response of species' iWUE to minimum and maximum temperature has been illustrated in [Supplementary Figure S4](#). **(D)** Linear regression between iWUE and atmospheric CO_2 concentration (Ca) for apple and pear trees. Apple is slightly more sensitive to changes in Ca (steeper slope), but Pear's iWUE is more tightly correlated with atmospheric CO_2 levels (higher R^2).

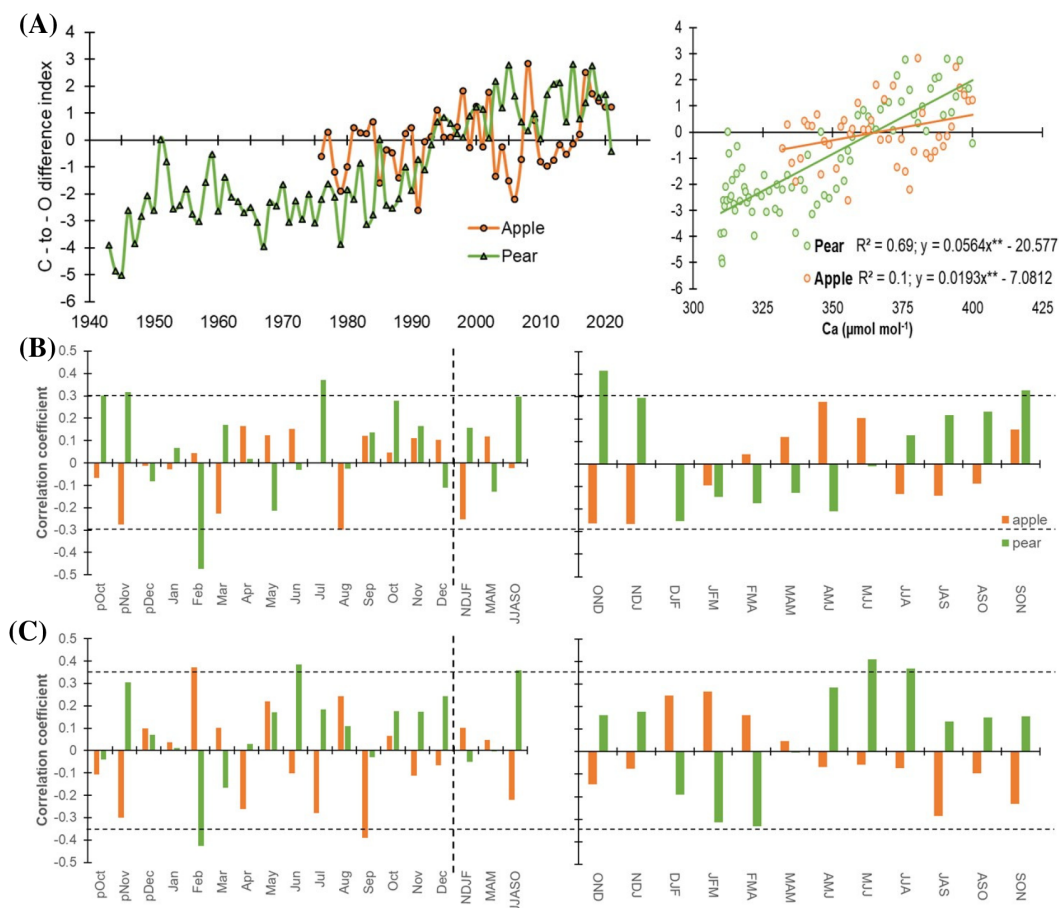


FIGURE 7

(A) Standardized carbon-to-oxygen isotope difference index for apple (orange) and pear (green) for the corresponding observation periods. Right panel plots the C-to-O difference index with atmospheric CO₂ levels (Ca) indicating physiological responses (through changes in stomatal conductance and photosynthetic capacity) to rising Ca. Slopes of both species are significant (** $p < 0.0001$). **(B)** Monthly (left panel) correlations between index time series of species and precipitation (1981-2021). The corresponding right panel indicates three-month moving correlation coefficients between them. **(C)** Monthly (left panel) and three-month moving (right panel) correlations between species' index time series and mean temperature (1988-2021). The dotted horizontal line indicates a 95% confidence level. The dashed vertical line delimits months with seasonal aggregates. Prefix "p" before the months denotes the months of the previous growth year. The response of species' index time series to minimum and maximum temperature has been illustrated in [Supplementary Figure S5](#).

improvement in photosynthetic assimilation. In recent decades (2000-2021), the overall trend remained positive, with a few dips indicating brief periods of moisture stress and reduced photosynthetic efficiency. The analysis suggests an overall improvement in photosynthetic capacity over the studied periods, with more frequent and sustained positive index values in recent decades in both species. This trend reflects adaptive physiological responses to changing environmental conditions including the CO₂ fertilization effect in the Italian Alps. However, both species exhibit notable year-to-year variability, highlighting the influence of inter-annual climatic variations on tree physiology and productivity.

Previously, we observed species-specific responses of *i*WUE to atmospheric CO₂ (Ca), with pear trees exhibiting lower *i*WUE and a higher regression coefficient ($R^2 = 0.91$) compared to apple trees ($R^2 = 0.76$) (Figures 6A, D). To further explore these differences, we plotted species' C-to-O difference indices against Ca (Figure 7A). The slope of pear trees (0.056, $p < 0.001$) with respect to apple trees (0.019, $p < 0.001$) suggests a stronger physiological response to

increased CO₂, with clear changes in stomatal conductance and photosynthetic activity (Figure 7A). Further, a much higher R^2 value for pear trees (69%) indicates that a significant portion of the changes in stomatal conductance and photosynthetic activity can be explained by changes in CO₂ concentration.

This suggests that pear trees' physiological conditions, as indicated by the index, are more closely tied to rising CO₂ levels compared to apple trees. The weak slope and low regression coefficient suggest that the physiological processes in the apple tree are primarily related to the stomatal regulation via soil moisture. Overall, our analysis revealed a significantly higher correlation for pear trees ($r = 0.83$, $p < 0.0001$) than for apple trees ($r = 0.32$, $p < 0.05$). These results suggest that apple trees may have reached a threshold in their ability to increase water use efficiency as CO₂ levels rise, while pear trees continue to show a stronger response. This could explain the differential responses of these two tree species to changing environmental conditions, including the CO₂ fertilization effect.

Cross-correlations with hydroclimatic variables were further performed to gain insights into the combined responses for the index series of the species. Response analyses clearly indicate that precipitation has a minimal impact on isotope-inferred ecophysiological processes, except for the pear trees which show a significant positive correlation during peak growing season (Figure 7B). Similarly, index – mean temperature relationship was significant only for the pear trees that only during peak growing season (Figure 7C). Both Pearson and 3-month moving correlations between minimum/maximum temperature and species index series have been detailed in the supplementary figure (Supplementary Figures S5A, B). These results demonstrate hydroclimate and ecophysiological relationships in these energy-limited ecosystems.

4 Conclusion

This study utilized unique old growth veteran apple and pear trees from energy-limited alpine valleys of the Italian Alps (a major national production center) to investigate climate-scale physiological responses. Results broadly indicate a species-coherent behavior and trends in $\delta^{18}\text{O}$ and processes such as *i*WUE, carbon discrimination ($\Delta^{13}\text{C}$) and intercellular CO_2 concentration (*C*_i). Importantly, results suggest a similar physiological response of tree species to atmospheric CO_2 rise. A significant increase in *i*WUE has been observed in recent decades, primarily driven by the CO_2 -fertilization effect. Dual isotope analyses ($\delta^{18}\text{O}$ – $\delta^{13}\text{C}$) confirmed that the recent rise in *i*WUE is due to increased carbon assimilation rather than reduced evapotranspiration. The analyses also highlight common inter-annual variability in carbon assimilation across both species, with some site- and species-specific responses. Among the major climatic controls on ecophysiological processes, precipitation has minimal impact in this moist, energy-limited ecosystem. Statistical and climate response function analyses further revealed that, besides CO_2 -fertilization, the second most important environmental driver of ecophysiological processes is the minimum temperature during the growing season. We believe that such long-term records could be valuable for fine-tuning land surface models to account for the combined effects of CO_2 -fertilization and climate impact.

Data availability statement

The raw data supporting the conclusions of this article will be made available by the authors, without undue reservation.

Author contributions

NS: Formal analysis, Investigation, Methodology, Conceptualization, Data curation, Writing – original draft. MT: Data curation, Investigation, Supervision, Validation, Visualization, Writing – review & editing. ET: Data curation, Investigation,

Validation, Visualization, Writing – review & editing, Methodology. LM: Investigation, Methodology, Visualization, Writing – review & editing, Formal analysis, Supervision.

Funding

The author(s) declare financial support was received for the research, authorship, and/or publication of this article. The study received main support from the EUREGIO funded ASTER project, EGTC European Region Tyrol-South Tyrol Trentino—IPN 101-32 and Austrian Science Fund (FWF) and was partially supported by the CarboST project funded by the Autonomous Province of Bolzano-Bozen.

Acknowledgments

The authors thank the Department of Innovation, Research, University and Museums of the Autonomous Province of Bozen/Bolzano for covering the Open Access publication costs. We are grateful to G. Battipaglia for her support for the stable isotope analyses that were carried out at the Università degli studi della Campania “L. Vanvitelli” Dipartimento di Scienze e Tecnologie Ambientali Biologiche e Farmaceutiche, Caserta, Italy. The authors also thanks W. Drahorad and R. Stainer for making possible the sampling of the old apple and pear trees.

Conflict of interest

The authors declare that the research was conducted in the absence of any commercial or financial relationships that could be construed as a potential conflict of interest.

The author(s) declared that they were an editorial board member of Frontiers, at the time of submission. This had no impact on the peer review process and the final decision.

Publisher's note

All claims expressed in this article are solely those of the authors and do not necessarily represent those of their affiliated organizations, or those of the publisher, the editors and the reviewers. Any product that may be evaluated in this article, or claim that may be made by its manufacturer, is not guaranteed or endorsed by the publisher.

Supplementary material

The Supplementary Material for this article can be found online at: <https://www.frontiersin.org/articles/10.3389/fpls.2024.1471415/full#supplementary-material>

References

- Adams, M. A., Buckley, T. N., and Turnbull, T. L. (2020). Diminishing CO₂-driven gains in water-use efficiency of global forests. *Nat. Climate Change* 10, 466–471. doi: 10.1038/s41558-020-0747-7
- Auzmendi, I., Marsal, J., Girona, J., and Lopez, G. (2013). Daily photosynthetic radiation use efficiency for apple and pear leaves: seasonal changes and estimation of canopy net carbon exchange rate. *Eur. J. Agron.* 51, 1–8. doi: 10.1016/j.eja.2013.05.007
- Babst, F., Alexander, M. R., Szejner, P., Bouriaud, O., Klesse, S., Roden, J., et al. (2014). A tree-ring perspective on the terrestrial carbon cycle. *Oecologia* 176, 307–322. doi: 10.1007/s00442-014-3031-6
- Baker, J. C. A., Gloor, M., Spracklen, D. V., Arnold, S. R., Tindall, J. C., Clerici, S. J., et al. (2016). What drives interannual variation in tree ring oxygen isotopes in the Amazon? *Geophysical Res. Lett.* 43, 11–831. doi: 10.1002/2016GL071507
- Barbour, M. M. (2007). Stable oxygen isotope composition of plant tissue: a review. *Funct. Plant Biol.* 34, 83–94. doi: 10.1071/FP06228
- Battipaglia, G., Saurer, M., Cherubini, P., Calfapietra, C., McCarthy, H. R., Norby, R. J., et al. (2013). Elevated CO₂ increases tree-level intrinsic water use efficiency: Insights from carbon and oxygen isotope analyses in tree rings across three forest FACE sites. *New Phytol.* 197, 544–554. doi: 10.1111/nph.2012.197.issue-2
- Belmecheri, S., and Lavergne, A. (2020). Compiled records of atmospheric CO₂ concentrations and stable carbon isotopes to reconstruct climate and derive plant ecophysiological indices from tree rings. *Dendrochronologia* 63, 125748. doi: 10.1016/j.dendro.2020.125748
- Core, R. (2015). *Team. R: a language and environment for statistical computing*. R Foundation for Statistical Computing, Vienna.
- Farquhar, G. D., Cernusak, L. A., and Barnes, B. (2007). Heavy water fractionation during transpiration. *Plant Physiol.* 143, 11–18. doi: 10.1104/pp.106.093278
- Farquhar, G. D., O'Leary, M. H., and Berry, J. A. (1982). On the relationship between carbon isotope discrimination and the intercellular carbon dioxide concentration in leaves. *Funct. Plant Biol.* 9, 121–137. doi: 10.1071/PP9820121
- Frank, D. C., Poulter, B. T., Saurer, M. A., Esper, J. A., Huntingford, C. T., Helle, G. F., et al. (2015). Water-use efficiency and transpiration across European forests during the Anthropocene. *Nature Climate Change* 5(6), 579–583.
- Gagen, M., Battipaglia, G., Daux, V., Duffy, J., Dorado-Liñán, I., Hayles, L. A., et al. (2022). "Climate signals in stable isotope tree-ring records," in *Stable Isotopes in Tree Rings: Inferring Physiological, Climatic and Environmental Responses* (Springer International Publishing, Cham), 537–579.
- García-Hidalgo, M., García-Pedrero, Á., Colón, D., Sangüesa-Barreda, G., García-Cervigón, A. I., López-Molina, J., et al. (2022). CaptuRING: A do-it-yourself tool for wood sample digitization. *Methods Ecol. Evol.* 13, 1185–1191. doi: 10.1111/2041-210X.13847
- Gessler, A., Ferrio, J. P., Hommel, R., Treydte, K., Werner, R. A., and Monson, R. K. (2014). Stable isotopes in tree rings: towards a mechanistic understanding of isotope fractionation and mixing processes from the leaves to the wood. *Tree Physiol.* 34, 796–818. doi: 10.1093/treephys/tpu040
- Giannarchi, F., Cherubini, P., Pretzsch, H., and Tonon, G. (2017). The increase of atmospheric CO₂ affects growth potential and intrinsic water-use efficiency of Norway spruce forests: insights from a multi-stable isotope analysis in tree rings of two Alpine chronosequences. *Trees* 31, 503–515. doi: 10.1007/s00468-016-1478-2
- Gimeno, T. E., Campany, C. E., Drake, J. E., Barton, C. V., Tjoelker, M. G., Ubierna, N., et al. (2021). Whole-tree mesophyll conductance reconciles isotopic and gas-exchange estimates of water-use efficiency. *New Phytol.* 229, 2535–2547. doi: 10.1111/nph.v229.5
- Gong, X. Y., Ma, W. T., Yu, Y. Z., Fang, K., Yang, Y., Tcherkez, G., et al. (2022). Overestimated gains in water-use efficiency by global forests. *Global Change Biol.* 28, 4923–4934. doi: 10.1111/gcb.v28.16
- Huang, R., Xu, C., Griesinger, J., Feng, X., Zhu, H., and Bräuning, A. (2024). Rising utilization of stable isotopes in tree rings for climate change and forest ecology. *J. Forestry Res.* 35, 13. doi: 10.1007/s11676-023-01668-5
- Hyvönen, R., Ågren, G. I., Linder, S., Persson, T., Cotrufo, M. F., Ekblad, A., et al. (2007). The likely impact of elevated [CO₂], nitrogen deposition, increased temperature and management on carbon sequestration in temperate and boreal forest ecosystems: a literature review. *New Phytol.* 173 (3), 463–480. doi: 10.1111/j.1469-8137.2007.01967.x
- Kahmen, A., Sachse, D., Arndt, S. K., Tu, K. P., Farrington, H., Vitousek, P. M., et al. (2011). Cellulose δ¹⁸O is an index of leaf-to-air vapor pressure difference (VPD) in tropical plants. *Proc. Natl. Acad. Sci.* 108, 1981–1986. doi: 10.1073/pnas.1018906108
- Lehmann, M. M., Goldsmith, G. R., Schmid, L., Gessler, A., Saurer, M., and Siegwolf, R. T. (2018). The effect of ¹⁸O-labelled water vapour on the oxygen isotope ratio of water and assimilates in plants at high humidity. *New Phytol.* 217, 105–116. doi: 10.1111/nph.2018.217.issue-1
- Lin, W., Barbour, M. M., and Song, X. (2022). Do changes in tree-ring δ¹⁸O indicate changes in stomatal conductance? *New Phytol.* 236 (3), 803–808. doi: 10.1111/nph.18431
- Ma, W. T., Tcherkez, G., Wang, X. M., Schäufele, R., Schnyder, H., Yang, Y., et al. (2021). Accounting for mesophyll conductance substantially improves ¹³C-based estimates of intrinsic water-use efficiency. *New Phytol.* 229, 1326–1338. doi: 10.1111/nph.v229.3
- Mathias, J. M., and Thomas, R. B. (2021). Global tree intrinsic water use efficiency is enhanced by increased atmospheric CO₂ and modulated by climate and plant functional types. *Proc. Natl. Acad. Sci.* 118, e2014286118. doi: 10.1073/pnas.2014286118
- McCarroll, D., and Loader, N. J. (2004). Stable isotopes in tree rings. *Quaternary Sci. Rev.* 23, 771–801. doi: 10.1016/j.quascirev.2003.06.017
- Nock, C. A., Baker, P. J., Wanek, W., Leis, A., Grabner, M., Bunyavejchewin, S., et al. (2011). Long-term increases in intrinsic water-use efficiency do not lead to increased stem growth in a tropical monsoon forest in western Thailand. *Global Change Biol.* 17, 1049–1063. doi: 10.1111/j.1365-2486.2010.02222.x
- Panthi, S., Fan, Z. X., van der Sleen, P., and Zuidema, P. A. (2020). Long-term physiological and growth responses of Himalayan fir to environmental change are mediated by mean climate. *Global Change Biol.* 26, 1778–1794. doi: 10.1111/gcb.14910
- Peñuelas, J., Canadell, J. G., and Ogaya, R. (2011). Increased water-use efficiency during the 20th century did not translate into enhanced tree growth. *Global Ecol. Biogeogr.* 20, 597–608. doi: 10.1111/j.1466-8238.2010.00608.x
- Rahman, M., Islam, M., Gebrekirstos, A., and Bräuning, A. (2020). Disentangling the effects of atmospheric CO₂ and climate on intrinsic water-use efficiency in South Asian tropical moist forest trees. *Tree Physiol.* 40, 904–916. doi: 10.1093/treephys/tpaa043
- Roden, J. S., Bowling, D. R., McDowell, N. G., Bond, B. J., and Ehleringer, J. R. (2005). Carbon and oxygen isotope ratios of tree ring cellulose along a precipitation transect in Oregon, United States. *J. Geophysical Res.: Biogeosci.* 110. doi: 10.1029/2005JG000033
- Saurer, M. A., Spahni, R. F., Frank, D. C., Joos, F. L., Leuenberger, M. L., Loader, N. J., et al. (2014). Spatial variability and temporal trends in water-use efficiency of European forests. *Global Change Biology* 20 (12), 3700–3712.
- Scheidegger, Y., Saurer, M., Bahn, M., and Siegwolf, R. (2000). Linking stable oxygen and carbon isotopes with stomatal conductance and photosynthetic capacity: a conceptual model. *Oecologia* 125, 350–357. doi: 10.1007/s004420000466
- Schollaen, K., Baschek, H., Heinrich, I., Slotta, F., Pauly, M., and Helle, G. (2017). A guideline for sample preparation in modern tree-ring stable isotope research. *Dendrochronologia* 44, 133–145. doi: 10.1016/j.dendro.2017.05.002
- Siegwolf, R. T., Lehmann, M. M., Goldsmith, G. R., Churakova, O. V., Mirande-Ney, C., Timoveeva, G., et al. (2023). Updating the dual C and O isotope-Gas-exchange model: A concept to understand plant responses to the environment and its implications for tree rings. *Plant Cell Environ.* 46, 2606–2627. doi: 10.1111/pce.14630
- Stenger, A., Harou, P., and Navrud, S. (2009). Valuing environmental goods and services derived from the forests. *J. For. Economics* 15, 1–14. doi: 10.1016/j.jfe.2008.03.001
- Van Der Sleen, P., Groenendijk, P., Vlam, M., Anten, N. P., Boom, A., Bongers, F., et al. (2015). No growth stimulation of tropical trees by 150 years of CO₂ fertilization but water-use efficiency increased. *Nat. Geosci.* 8, 24–28. doi: 10.1038/ngeo2313
- Walker, A. P., De Kauwe, M. G., Bastos, A., Belmecheri, S., Georgiou, K., Keeling, R. F., et al. (2021). Integrating the evidence for a terrestrial carbon sink caused by increasing atmospheric CO₂. *New Phytol.* 229, 2413–2445. doi: 10.1111/nph.v229.5
- Wang, W., Liu, X., Xu, G., Treydte, K., Shao, X., Qin, D., et al. (2019). CO₂ fertilization confounds tree-ring records of regional hydroclimate at northeastern Qinghai-Tibetan Plateau. *Earth Space Sci.* 6, 730–740. doi: 10.1029/2018EA000529
- Waterhouse, J. S., Switsur, V. R., Barker, A. C., Carter, A. H. C., Hemming, D. L., Loader, N. J., et al. (2004). Northern European trees show a progressively diminishing response to increasing atmospheric carbon dioxide concentrations. *Quaternary Sci. Rev.* 23, 803–810. doi: 10.1016/j.quascirev.2003.06.011
- Wieser, G., Oberhuber, W., Gruber, A., Leo, M., Matyssek, R., and Grams, T. E. E. (2016). Stable water use efficiency under climate change of three sympatric conifer species at the alpine treeline. *Front. Plant Sci.* 7, 799. doi: 10.3389/fpls.2016.00799